Application of Precision Magnetic Measurements for Control of the Duke Storage Ring*

B. Burnham, V.N. Litvinenko, Y. Wu
Duke University Free Electron Laser Laboratory
Box 90319 Duke University Durham, NC 27708-0319

Presented at the 1995 Particle Accelerator Conference, May 1 - 5 in Dallas, Texas USA

I. INTRODUCTION

The 1 GeV Duke FEL storage ring is dedicated to drive UV and VUV free electron laser devices. Specifics of this ring include the use of combined function magnets: quadrupole-sextupole and dipole-sextupole. The use of combined function magnets is necessitated by the close spacing of magnetic elements. A discussion on the measurement procedures of these magnets is included in this paper, as well as the data analysis used to create a viable control system for the combined function magnets.

The design of the Duke storage ring was driven by the requirement to use existing hardware manufactured for the original ring design at Stanford. The original design called for the use of "nose" and "dimple" endpieces attached to the dipoles as the main fixed strength sextupole source. In addition, adjustable sextupole magnets were placed in an 18 cm gap between dipoles and arc quadrupoles. In that design the distance between magnetic poles of dipoles, quadrupoles, and sextupoles was less than 2 cm. It was no surprise that this design uncovered major asymmetric saturation of dipoles and sextupoles. Saturation would cause intolerable orbit distortion and high order nonlinearities in the magnetic field.

To solve these problems we decided to:

a) replace odd asymmetric endpieces with smooth and symmetric ones;
b) remove discrete sextupoles which were saturated anyway;
c) create necessary sextupole moments in the quadrupoles using asymmetric excitation;
d) place fixed strength sextupole shims in the center of the dipoles.

II. MEASUREMENT PROCEDURES

Magnetic measurements of all magnets were performed prior to installation on the storage ring. In order to facilitate fast data acquisition of large data sets of magnetic fields accurately we made use of a Hall probe array. Details of the array and its electronics can be found in a previous paper [1].

The high resolution of the array and its electronics yield a magnetic measurement accuracy of better than one part in 10,000 and we can make a two dimensional map with only one pull through each magnet. A set of tracks are used for the precise positioning of the array in each magnet. Since the magnet lattice includes closely spaced elements it is important that all measurements be taken in a real environment. The magnet test bed at Duke has room to place neighboring magnets around the magnet under test as would be the case when the magnet is eventually placed into the storage ring. In this manner we can better understand the fringe field effects and cross-talk of closely spaced elements.

Each dipole magnet is measured with one current ramp using small current increments, and four field maps. Each arc quadrupole is measured with three asymmetric current ramps and five field maps. We use the maps to evaluate magnetic length dependence on current. Then we use interpolated values of magnetic length in combination with the ramping data for precise characterization of magnetic moments.

The normalization curves used to standardize each magnet before measurement are now also used prior to operating the storage ring. This is so that the magnets resemble as closely as possible the same condition they were in when they were measured on the test bed.

To insure consistency with magnetic measurements we calibrated all power supplies and current sensors (shunts, DCCT) using sets of equipment used for magnetic measurements. Controls use individual second order polynomial fits for all power supplies.

III. COMBINED FUNCTION QUADRUPOLES

The arc combined function quadrupoles are wired so that we can independently control the quadrupole and sextupole moments. Quadrupole coils are fed by an individually controlled power supply. An individually controlled shunt regulator is connected to the pair of coils on the inner side of the ring. With no current in the shunt regulator all coils have the same excitation and there is a pure quadrupole moment. By shunting the inner coils we excite dipole and sextupole moments in the magnet. The dipole moment offsets the magnetic center of the quadrupole-sextupole. We have therefore designed the ring so that the electron orbit will pass through this new magnetic center, 2 mm for the design value of the sextupoles.

We have taken large data sets of all of the quadrupole magnets in field mappings and current rampings and created a computer routine to fit the multipole moments using spline interpolation in multi-dimensional space. These data are used in the control system, described below, to achieve the desired strengths in the quadrupole. Graphs showing current settings and field distributions can be found in [1].

The pole tips of the arc quadrupoles (inner radius = 2 cm) have shape corrections to compensate for fringe effects and finite size of the poles. These corrections work as well for combined function quadrupoles. Figure 4 of Reference 1

---

*This work supported by U.S. Air Force Office of Scientific Research grant F49620-93-1-0590 and U.S. Army Space & Strategic Defense Command contract DASG60-89-C-0028.

shows a plot of the integrated moments above sextupole for both the central part of the magnet and the fringe fields: one curve is the integral of the fields inside the magnet steel without edges, the other for the fringe field. The two very nearly cancel out overall higher order moments. Thus, combined function quadrupoles with asymmetric excitation are nearly perfect; the lowest moment in the integrated field is dodecapole.

IV. COMBINED FUNCTION DIPOLES

We replaced the odd shaped nose and dimple dipole end pieces with new parallel edge smooth symmetric end pieces required to extend dipole magnetic length. This allows us to reach a symmetric magnetic field of 20.5 kGs with excellent quality (15.9 kGs is required for 1 GeV operation). We have devised a way to make the dipole magnets combined function while maintaining a higher level of symmetry by introducing thin steel shim stock in the center of the magnet. These fixed strength sextupoles are not a necessity for the Duke ring. We decided to introduce them in order to simplify quadrupole alignment by maintaining a magnetic center offset of 2 mm in both focusing and defocusing arc quadrupoles. This extra "bump" creates a defocusing sextupole field of the desired strength as shown in Figure 1. In this figure, the peak is 60 Gauss above the baseline field of 3.96 kGs. The steel

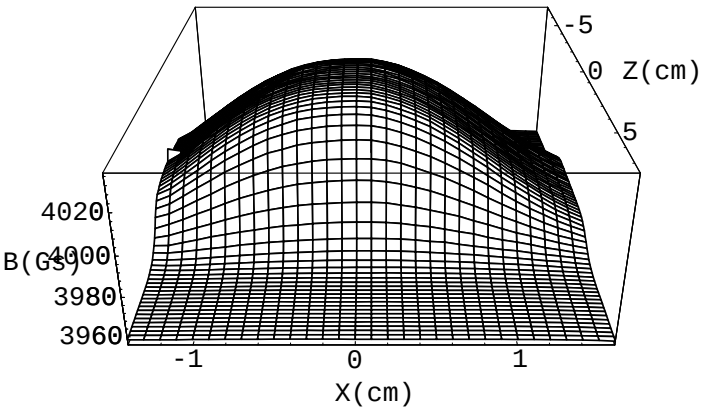

Figure 1. Field map of dipole thin shim stock.

shims themselves are mounted on aluminum strips, so the whole unit is easily replaced if desired. The 0.005 inch thick steel shim stock measures only 6.4 cm long by 2.5 cm wide in a 33 cm long magnet. The measured sextupole moment as a function of longitudinal distance is shown in [1].

V. OTHER MAGNETS

We use standard quadrupoles (inner radius = 3 cm) in the ring straight sections, linac, and linac-to-ring transport channel. These magnets also pass through standard ramping and magnetic measurements. Data analysis for these magnets is much simpler than for the combined function quadrupoles.

The Lambertson type septum magnet used on the Duke ring was measured in a similar manner employing a specially designed curved track to follow the expected orbit of the electron beam. Integrated strengths were calculated from the resulting field ramps and maps.

The data of the measured strengths of all steering dipoles, trim coils, and other small magnets are also used for computer control.

VI. ANALYSIS AND CONTROL

Dipoles:

We have used a special program to track the particles through five 2-D field maps to calculate dipole magnetic lengths as a function of current. Combined with measured ramping curves, the data provides us with individual integrated characteristics of the dipole and sextupole moments:

$$D_i = f_i(I)$$
$$S_i = g_i(I) \qquad (1)$$

Spline fits interpolate these functions between measured points.

All bending magnets and injection chicanes are powered by one 560 kW PEI power supply. For control we use the total dipole moment dependence

$$D_a(I) = \sum_i D_i(I) \qquad (2)$$

This gives us the particle momentum as a function of the PEI current:

$$pc(MeV) = \frac{0.29979}{2\pi} \sum_i D_i(I)[kGs \cdot cm] \qquad (3)$$

The settings of other magnets are based on the ring energy and design lattice.

To insure that each of the 40 dipoles turns the beam 9° we use individual dipole trim currents:

$$\Delta D_i(I_{trim}) = \frac{D_a(I)}{40} - D_i(I) \qquad (4)$$

Individual dipole trims are also used for closed orbit correction and are calibrated in milliradians as are all steering and quadrupole trim magnets.

Standard Quadrupoles:

For the standard quadrupoles we analyzed the integrated quadrupole dependence as a function of coil current:

$$Q_i = A_i(I). \qquad (5)$$

We used the ramping data taken in the center of the magnet along with five field maps to calculate the quadrupole moment versus current curves. Then we use individual cubic spline fits to interpolate between measurement points.

Combined Function Quadrupoles:

Analysis of the combined function quadrupoles assumed that the pole tips are non-saturated and that the filed is a superposition of quadrupole and dipole-sextupole fields. Computer models and data analysis showed that the fields could be fit by the following forms:

$$Q_g = A(\bar{I}) + B(\bar{I})(\Delta I)^2$$
$$S = S_g = C(\bar{I})(\Delta I) \qquad (6)$$
$$D_g = \alpha S$$

where Q_g, S_g, and D_g are the respective quadrupole, sextupole, and dipole moments in the geometric center of the

magnet; Q, S, and D are the respective moments at the magnetic center; A, B, and C are functions of the average current $\bar{I}$ = (I_1 + I_2) / 2 through the two halves of the quadrupole, and the current separation is ΔI = (I_1 - I_2) / 2. The dipole and sextupole moments are both odd multipole moments and hence may be closely related. This simple relation is indicated by the coefficient α on the dipole moment. This is due to the fact that the pole tips are not saturated. Saturation occurs farther up the neck of the yoke.

Substitution for ΔI from the equation for S_g into the equation for Q_g shows that the quadrupole moment is proportional to S_g^2. In figure 2 we plot the quadrupole versus sextupole moments where each data point represents a different separation current, but the average current is the same.

The graph shown in figure 2 is repeated for every average current setting used in the measurements. The DC and second order terms of the parabolic fit coefficients are saved as a function of average current. These two functions, then, are A($\bar{I}$) and B($\bar{I}$) and are shown graphically in figure 3. The central values for Q and S calculated from the curves in figure 3 are related to the integrated moments simply by multiplying the central value by the effective length of the magnet. The effective length is calculated from the two dimensional field maps and is very nearly a linear function of average current, which is natural for quadrupoles with no chamfers.

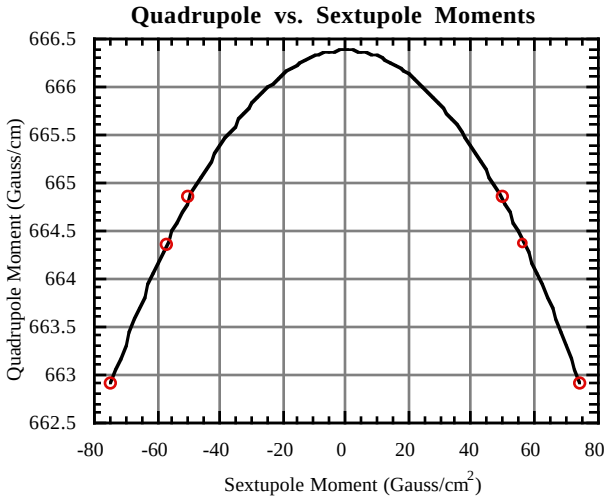

Figure 2. Plot and parabolic fit of quadrupole versus sextupole moments for given average current.

A curve is similarly generated for the sextupole moment coefficient C($\bar{I}$) using a linear fit to the sextupole moment versus current separation. The dipole proportionality constant α is also determined from the mapping data. These assumptions are confirmed by detailed analysis of magnetic measurement data and computer simulations.

The shift of magnetic center, defined as x_0, is found by a simple change of coordinate system. By definition the dipole

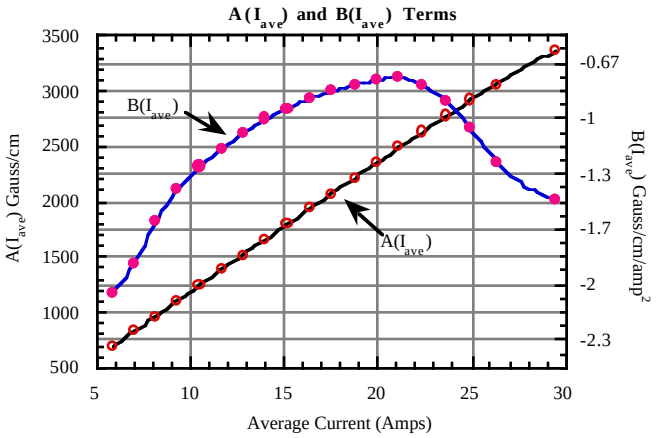

Figure 3. Coefficient curves with spline fits.

moment at magnetic center is zero, and the geometric and magnetic center values of quadrupole moment are related by

$$Q_g = Q - Sx_0 = \sqrt{Q^2 - 2\alpha S^2} \quad (7)$$

Substitution back into the first of equation 6 gives

$$A(\bar{I}) + \frac{B(\bar{I})}{C(\bar{I})^2} S^2 - \sqrt{Q^2 - 2\alpha S^2} = 0 \quad (8)$$

Using this formula it is straightforward to invert the functions of the graph of Figure 3 to find

$$\bar{I} = f(Q,S)$$

$$\Delta I = \frac{S}{C(f(Q,S))} \quad (9)$$

VII. CONCLUSIONS

The effort spent on magnetic measurements and applications which use the magnetic measurement data for control paid off in the end. The commissioning of the Duke storage ring was a great success. We did not experience any problems storing electrons on the first try, or ramping the energy from 230 MeV to 1.1 GeV. All measured parameters of the ring, such as tunes and chromaticity, are very close to the design values [2].

Implementation of magnetic measurements for controls was provided by a set of programs using the EPICS control system and the Tcl-Tk scripting language[3]. Work is in progress to implement these controls at a lower level for greater speed.

VIII. REFERENCES

[1] B. Burnham, N. Hower, V. N. Litvinenko, J.M.J. Madey, Y. Wu, "Specific Features of Magnet Design for the Duke FEL Storage Ring" in Proceedings of the 1993 Particle Accelerator Conference, Washington, D.C., p. 2889.

[2] V. N. Litvinenko, et al., "Commissioning of the Duke Storage Ring", these proceedings.

[3] Y. Wu, et al., "The Duke Storage Ring Control System", these proceedings.